ELSEVIER

Polymer 41 (2000) 3745–3749

polymer

Structural and morphological aspects of some polymorphs of syndiotactic poly(*p*-methylstyrene)

P. Rizzo[a], O. Ruiz de Ballesteros[b], C. De Rosa[a], F. Auriemma[a,*], D. La Camera[a], V. Petraccone[a], B. Lotz[c]

[a]*Dipartimento di Chimica, Università degli Studi di Napoli, "Federico II", Via Mezzocannone, 4 80134 Naples, Italy*
[b]*Dipartimento di Chimica, Università degli Studi di Salerno, Via S. Allende, 84081 Baronissi (SA), Italy*
[c]*Institut Charles Sadron (CNRS-ULP) 6, rue Boussingault, 67083 Strasbourg, France*

Received 23 March 1999; received in revised form 3 May 1999; accepted 14 June 1999

Abstract

Novel data about the crystal morphology and the electron diffraction of syndiotactic poly(*p*-methylstyrene) (s-PPMS) in form I and in the clathrate forms including *o*-dichlorobenzene and tetrahydrofuran are presented. Preparative routes of s-PPMS samples in the various polymorphs suitable for electron microscopy and diffraction have been devised. This investigation provides data, unavailable in the past literature, helpful to get direct structural information and to better understand the ways of obtaining and stabilizing the various polymorphs.

Keywords: Syndiotactic poly(*p*-methylstyrene); Crystal morphology; Electron diffraction

1. Introduction

Syndiotactic poly(*p*-methylstyrene) (s-PPMS) presents a complex polymorphism: four different crystalline forms (named I, II, III and V), a mesomorphic form (IV) and several clathrate forms, including solvent molecules, have been observed so far [1–4]. As described in Ref. [1] s-PPMS does not crystallize by cooling from the melt or by annealing the amorphous phase; crystallization may be induced through casting procedures, precipitation from solution or solvent-induced crystallization from the amorphous state. The obtaining of crystalline and clathrate forms depends on solvent, crystallization techniques or other parameters (casting-temperature, nature of the non-solvent during precipitation, etc.).

Two classes of clathrates, named α and β, have been obtained [5]. The two classes differ by the nature of the included guest molecules, mostly related to their steric hindrance illustrated by the presence or not of *ortho* substituents on the ring structure. For instance, solvents such as *o*-dichlorobenzene, *o*-chlorophenol, *o*-xylene and *N*-methyl-2-pyrrolidone induce the crystallization of α class clathrates, whereas solvents such as tetrahydrofuran, benzene, 1,4-dioxane, cyclohexane and cyclohexanone induce crystallization of β class clathrates.

In this paper we report novel data (optical and electron microscopy and electron diffraction), on single crystals and spherulites of s-PPMS in the various crystalline forms. Preparative routes of single crystals of s-PPMS in the clathrate forms and in form I have been devised. The new structural information, unavailable in the past literature, will help to better understand the ways of obtaining and stabilizing the various polymorphs.

2. Experimental procedures

The s-PPMS sample used in this investigation was synthesized following the procedure already described in Ref. [6]. The fraction of rrrr pentads, evaluated by ^{13}C NMR, was higher than 95%.

Thin films of the polymer were obtained by evaporation of the solvent, by smearing a drop of a solution (0.4 wt.%, in toluene) on cleaved mica and/or on glass microscope cover slides. The films heated up to 230°C were quenched at room temperature and subsequently exposed to organic solvent vapors in an oven at about 50°C for one day or more.

The pure organic solvents used were *o*-dichlorobenzene (*o*-DCB) and tetrahydrofuran (THF), which induce formation of clathrates belonging to α and β classes, respectively.

* Corresponding author.

0032-3861/00/$ - see front matter
PII: S0032-3861(99)00440-1

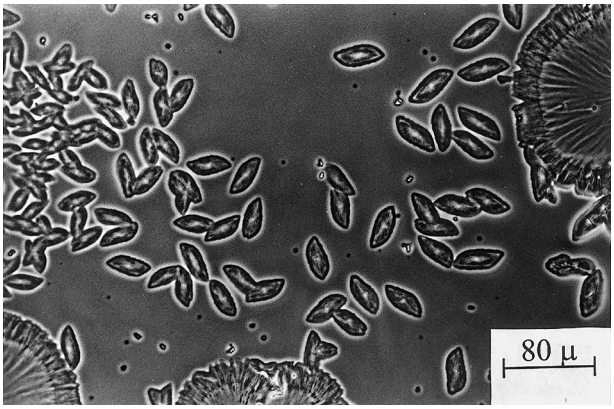

Fig. 1. Optical micrograph (phase contrast) of flat radial growth and single crystals of the clathrate form of s-PPMS including *o*-DCB produced by diffusion of the solvent in thin film.

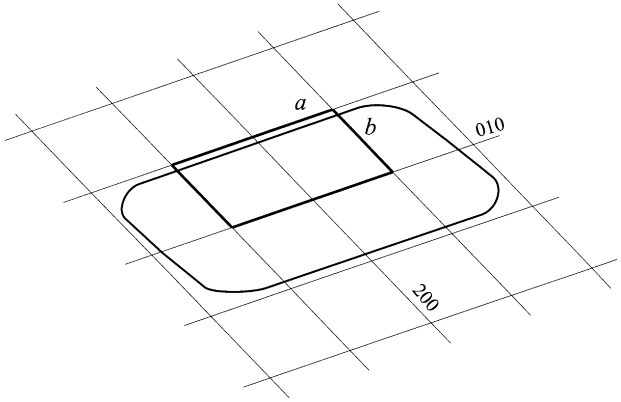

Scheme 1. Relative orientation of the unit cell and the single crystal of the clathrate form of s-PPMS including *o*-DCB. The traces of the (010) and (200) Miller planes are indicated.

Thermal treatments were performed using a Mettler FP80 microscope heating stage.

Before examination, the samples were subjected to conventional Pt–C shadowing and carbon backing.

Electron microscopy and diffraction was performed with a Philips CM12 electron microscope operating at 120 kV.

3. Results and discussion

3.1. α Class of s-PPMS clathrates: the clathrate including o-DCB

Single crystals of the clathrate including *o*-DCB (belonging to the α class) grown from dilute solutions are very small, do not present defined shapes and are cusped [7], most probably because *o*-DBC is not a good solvent for s-PPMS and crystallization takes place in a liquid–liquid phase separated system [8]. On the contrary, single crystals obtained by solvent diffusion in thin films are at least four times larger and have a lozenge shape.

Optical and electron micrographs of single crystals obtained by solvent diffusion in thin films are shown in Figs. 1 and 2A, respectively. Two corners of the lozenges are rounded, and as shown in Fig. 2A, the crystals are striped probably because of a partial loss of the solvent in the high vacuum of the electron microscope.

An electron diffraction pattern corresponding to the single crystal of Fig. 2A is shown in Fig. 2B. It is characterized by the presence of only a few sharp spots, with spacings $d = 10.43$, 10.24 and 9.61 Å. The crystals are probably disordered.

Based on the X-ray fiber and powder diffraction patterns of the s-PPMS clathrate including *o*-DCB molecules [4] and the electron diffraction pattern of Fig. 2B, a unit cell with $a = 23.4$ Å, $b = 11.8$ Å, $c = 7.7$ Å, $\gamma = 115°$ is proposed.

Accordingly, the above electron diffraction reflections can be indexed as 010, 200 and $\bar{2}10$, hence, the growing faces of the single crystals are parallel to the crystallographic (010) (longer face) and (200) (shorter face) planes, as illustrated in Scheme 1.

It is worth noting that the electron diffraction data allowed us to resolve the single peak and/or spot observed at $d = 10.56$ Å in the X-ray powder and fiber diffraction pattern [4], into two contributions corresponding to the 010 and 200 reflections at $d = 10.43$ and 10.24 Å, respectively.

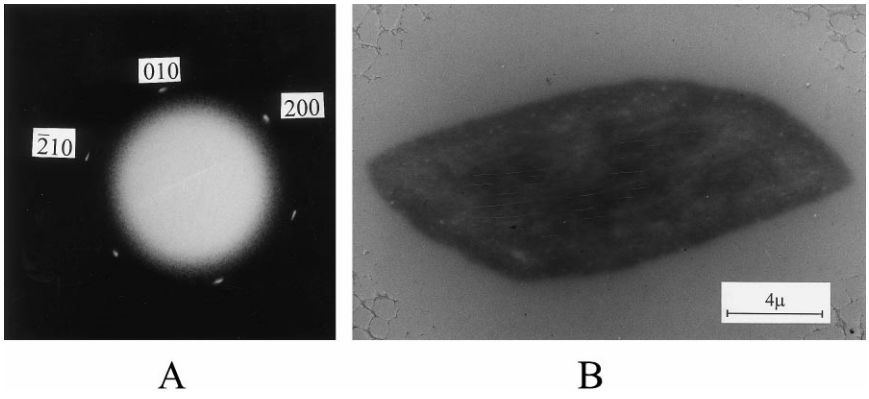

Fig. 2. Electron micrograph of a single crystal of the clathrate form of s-PPMS including *o*-DCB (A) and the corresponding electron diffraction pattern (B) in correct relative orientation. The indexing of the reflections refers to the hypothesis of the unit cell discussed in the text.

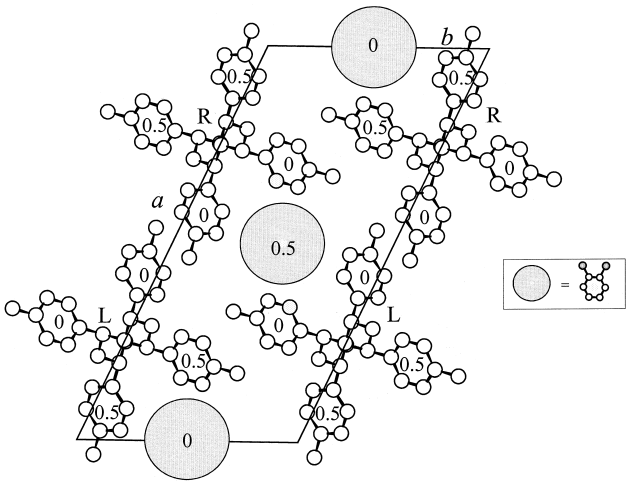

Fig. 3. Preliminary packing model of the crystal structure of the clathrate form of s-PPMS including *o*-DCB in the space group $P2_1/a$. The spaces in which the guest molecules are accommodated are indicated by filled circles. R, right-handed; L, left-handed helix. The approximate *z*/*c* fractional coordinates of the barycenters of the phenyl groups and of the guest molecules are also indicated.

A preliminary packing model of the crystal structure of this clathrate form, according to the space group $P2_1/a$, is shown in Fig. 3.

The differences in the relative intensities of the 010, 200 and $\bar{2}10$ reflections between the electron diffraction pattern (Fig. 2B) and the X-ray powder diffraction pattern (see Ref. [4, Fig. 5 and Table 2]) could be due to the loss of solvent. In fact, these reflections have nearly the same intensity in the electron diffraction pattern, whereas in the X-ray powder diffraction pattern the 010 and 200 reflections (single peak at $2\vartheta = 8.4°$) are much weaker than the $\bar{2}10$ one (peak at $2\vartheta = 9.2°$). Preliminary structure factor calculations, for the model of Fig. 3, have shown that the ratio between the sum of the intensities of 010 and 200 reflections and the intensity of the $\bar{2}10$ reflection increases with decreasing the occupation factor of the atoms of the guest molecules.

It is worth noting that in the clathrate structure of the β class [9] guest molecules occupy cavities around the two-fold screw axes of the lattice, whereas in the clathrate form including *o*-DCB molecules (α class), the cavities are around the inversion centers (see Fig. 3) as in the s-PS clathrates [10–12].

Work is in progress in our laboratories to clarify in detail the crystal structure of the clathrate form of s-PPMS containing *o*-DCB.

3.2. Form I

The crystalline polymorphs named forms I and II of s-PPMS may be obtained through suitable thermal treatments of the α and β class clathrates, respectively [4,5].

By heating up to 120°C the single crystals of the clathrate including *o*-DCB, transformation into form I occurs. Fig. 4A shows a single crystal of the *o*-DCB clathrate (Fig. 2A) after the heat treatment and Fig. 4B the corresponding electron diffraction pattern. From Fig. 4A it is apparent that the single crystals lose definition along the contour path and stripes become more conspicuous probably due to the further loss of solvent and/or as result of a lamellar thickening process.

Probably as a result of the phase transition, the single crystals break down; their electron diffraction patterns display arcs instead of spots (Fig. 4B).

Reflections characteristic of form I may nevertheless be recognized at $d = 11.79$, 5.82 and 5.44 Å (see for comparison Ref. [4], Table 4]).

3.3. β class of s-PPMS clathrates: the THF clathrate

We recall that for the β class clathrates of s-PPMS a structural model based on X-ray diffraction has been proposed in Ref. [9] in the case of the clathrate including THF molecules. According to Ref. [9] the crystal structure is characterized by a close packing of right- and left-handed helical chains alternating along the *a* axis, whereas the packing is less well defined along the *b* axis. This indicates the presence along the *b* axis of enough space to accommodate the THF molecules: two cavities are included in each unit cell, each cavity being able to accommodate up to two THF molecules related by the two-fold screw axes.

In the present set of experiments, diffusion of THF vapors

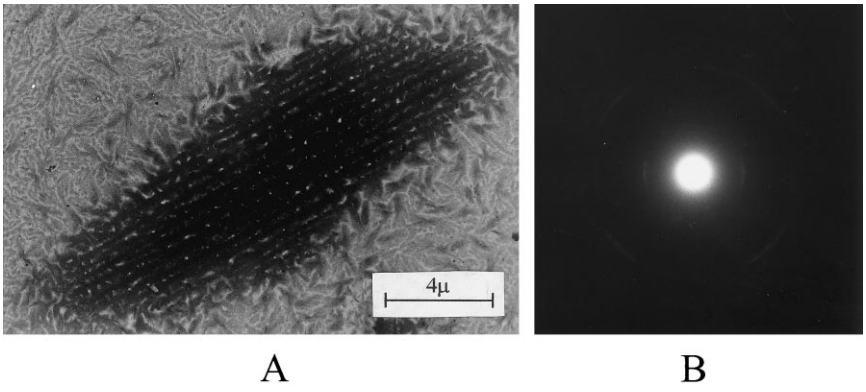

Fig. 4. Electron micrograph of a single crystal of form I of s-PPMS (A) and the corresponding electron diffraction pattern (B).

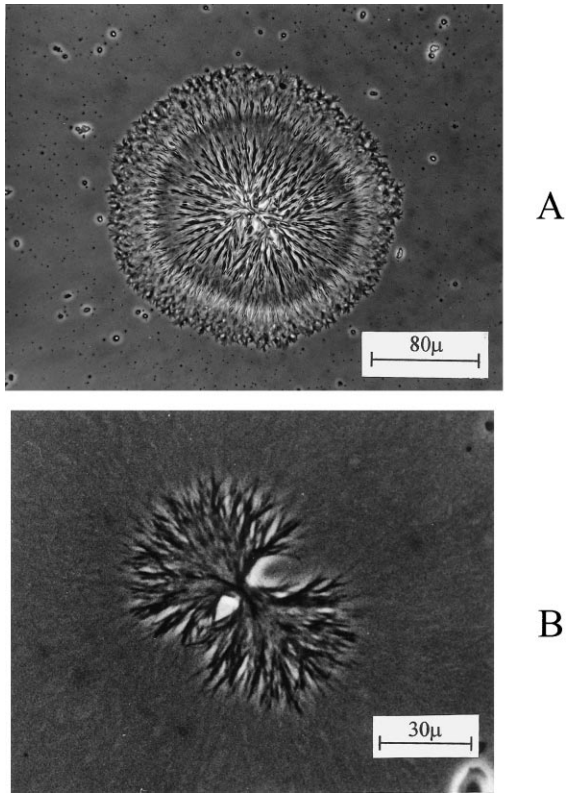

Fig. 5. Optical micrograph (phase contrast) of a spherulite (A) and of a partially grown spherulite (B) of the clathrate form of s-PPMS including THF.

in thin films of s-PPMS did not produce single crystals as in the case of *o*-DCB, but promoted growth of spherulites. Fig. 5A and B show the optical micrographs of spherulites of the clathrates including THF. The diameter of the spherulite of Fig. 5A is about 200 μm, whereas the growth of the spherulite in Fig. 5B was arrested. A close-up view of the latter spherulite reveals its lamellar organization. The electron diffraction pattern of a small portion of this spherulite, in which the lamellae are almost flat-on, is shown in Fig. 6.

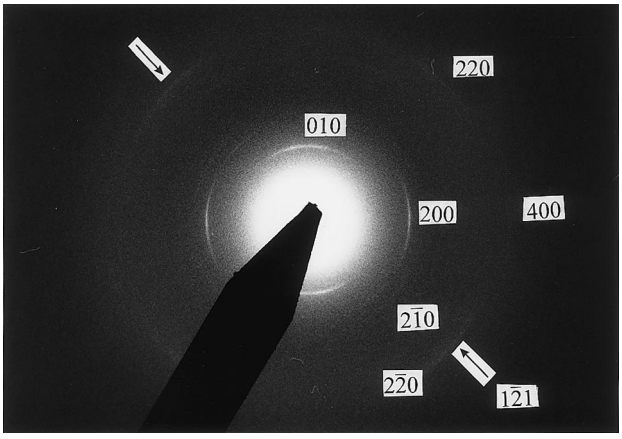

Fig. 6. Electron diffraction pattern of a small portion of the spherulite of Fig. 5 in which lamellae are flat-on.

Table 1
Bragg distances (d_{obs}) observed in the electron diffraction pattern of s-PPMS clathrates including THF, and calculated (d_{calc}) for the unit cell $a =$ 18.8 Å, $b = 12.7$ Å, $c = 7.7$ Å, $\gamma = 100°$ are reported. A qualitative evaluation of the observed intensities is also reported

d_{obs} (Å)	d_{cal} (Å)	*hkl*	I_o[a]
12.7	12.51	010	vs
9.3	9.26	200	s
8.23	8.15	2$\bar{1}$0	w
5.78	5.66	2$\bar{2}$0	w
4.88	4.81	220	m
4.90	4.86[b]	1$\bar{2}$1[b]	w
4.63	4.63	400	vw
4.20	4.11	410	w

[a] s, strong; m, medium; w, weak; vw, very weak.
[b] See comments in the text.

Several reflections (see Table 1) are observed: they are arced and correspond to the equatorial reflections in the X-ray fiber diffraction patterns of s-PPMS clathrates including THF reported in Ref. [9]. Note in Fig. 6 the presence of a reflection at $d = 4.90$Å (evidenced with an arrow in the figure), which could correspond to Miller indices $\bar{3}20$. Reflections with $h = 2n + 1$ are forbidden in the space group $P2_1/a$. It is worth noting, however, that a strong reflection corresponding to $d = 4.88$ Å exists on the first layer line in the X-ray fiber diffraction pattern (see Ref. [9, Fig. 1]). It is therefore probable that in the zone of the selected spherulite the crystals are not perfectly flat and as a result, first layer line reflections appear in the 001 electron diffraction pattern.

A slight discrepancy between the intensities observed in the electron and X-ray diffraction patterns is apparent. In fact, whereas in the electron pattern of Fig. 6 the 010 reflection appears stronger than the 200 one, it appears weaker in the X-ray fiber diffraction pattern of Ref. [9, Fig. 1]. This could be explained by a partial loss of solvent probably due to the high vacuum of the electron microscope. According to the proposed structural model [9] the intensity ratio between the 010 and the 200 reflections increases with decreasing occupation factor of the atoms of THF molecules.

In summary, the electron diffraction pattern of Fig. 6 is in good agreement with the crystal structure proposed for the clathrate including THF in Ref. [9] (unit cell parameters $a = 18.8$ Å, $b = 12.7$ Å, $c = 7.7$Å, $\gamma = 100°$, space group $P2_1/a$).

4. Concluding remarks

This paper reports novel morphological and structural information on various polymorphs of s-PPMS. Preparative routes of s-PPMS flat-on lamellae or single crystals in the various polymorphs suitable for electron diffraction and electron microscopy techniques have been devised. In

particular, form I and clathrates including *o*-DCB (belonging to the α class) and THF (β class) have been prepared.

Electron diffraction data provide direct structural information which strongly support earlier structural hypotheses based on X-ray diffraction data [4,9]. For the β class clathrate, electron diffraction data confirm the structure proposed in the literature for the clathrate with THF. For the α class clathrate, a unit cell is proposed for the *o*-DCB clathrate, which accounts both for electron diffraction data reported in this paper and for earlier X-ray diffraction data [4]. A preliminary packing model, based on packing energy and structure factors calculations, is proposed. According to this model, the guest molecules are located in cavities around the crystallographic inversion centers, as in the s-PS clathrate forms. This model differs from the β class s-PPMS clathrates, in which the guest molecules occupy cavities around the two-fold screw crystallographic axes.

Acknowledgements

This work was supported by the Ministero dell'Università e della Ricerca Scientifica e Tecnologica (PRIN 1998 titled "Stereoselective Polymerization: New Catalysts and New Polymeric Materials"). P.R. and F.A. thank the Consiglio Nazionale delle Ricerche of Italy and the Università di Napoli "Federico II" of Italy for the financial support of the short mobility research. O.R. also thanks the Università di Napoli "Federico II" of Italy for having furnished a fellowship.

References

[1] Iuliano M, Guerra G, Petraccone V, Corradini P, Pellecchia C. New Polymeric Mater 1992;3:133.
[2] Guerra G, Iuliano M, Grassi A, Rice DM, Karasz FE, Mc Knight W. Polym Commun 1991;32:430.
[3] Guerra G, Dal Poggetto F, Iuliano M, Manfredi C. Makromol Chem 1992;193:2413.
[4] De Rosa C, Petraccone V, Guerra G, Manfredi C. Polymer 1996;37:5247.
[5] Dell'Isola A, Floridi G, Rizzo P, Ruiz de Ballesteros O, Petraccone V. Macromol Symp 1997;114:243.
[6] Grassi A, Longo P, Proto A, Zambelli A. Macromolecules 1989;22:104.
[7] Khoury F, Passaglia E. Treatise of solid state chemistry, 3. New York: Plenum Press, 1976. p. 335–496 Chap. 6.
[8] Schaaf P, Lotz B, Wittmann JC. Polymer 1987;28:193.
[9] Petraccone V, La Camera D, Pirozzi B, Rizzo P, De Rosa C. Macromolecules 1998;31:5830.
[10] Chatani Y, Shimane Y, Inagaki T, Ijitsu T, Yukinari T, Shikuma H. Polymer 1993;34:1620.
[11] Chatani Y, Inagaki T, Shimane Y, Shikuma H. Polymer 1993;34:4841.
[12] De Rosa C, Rizzo P, Ruiz de Ballesteros O, Petraccone V, Guerra G. Polymer 1999;40:2103.